

Constructing Auxiliary Dynamics for Nonequilibrium Stationary States with Variational Monte-Carlo

Ushnish Ray* and Garnet Kin-Lic Chan†
Division of Chemistry and Chemical Engineering,
California Institute of Technology, Pasadena, CA 91125
(Dated: April 1, 2022)

We present a strategy to construct guiding distribution functions (GDFs) based on a variance minimization principle. This technique exploits the exact properties of eigenstates of the tilted operator used to compute large deviation functions. Auxiliary dynamics via GDFs is a viable route to mitigate the exponential growth of variance in Monte-Carlo estimators that arise in prototypical nonequilibrium systems. We demonstrate our techniques in two classes of problems. In the continuum, we show that GDFs can be constructed to study interacting driven diffusive systems where the efficiency can be improved by systematically incorporating higher order correlations. In the lattice, we use correlated product states as GDFs to study the 1D WASEP. We show that with modest resources we are able to compute the second order cumulant or susceptibility that captures the phase transition from a uniform transport to a traveling wave state in large systems. Our work extends the repertoire of tools needed to study properties of realistic systems.

Large deviation theory (LDT) is a framework that extends tools of equilibrium statistical mechanics to nonequilibrium systems [1]. Much of LDT is concerned with fluctuations of typical trajectories as they encode the information relevant to the physics of a particular system. The spectrum of these rare trajectories display fascinating behavior reminiscent of phase transitions, criticality, even suggesting universality. Recent work has been concerned with understanding such dynamical behavior in lattice systems such as simple exclusion processes [2–9], constrained kinetic models [10, 11], models of self-assembly [12–15], dissipative hydrodynamics [16, 17], in continuum systems in the form of driven or active Brownian particles [14, 18–27], as well as open quantum systems [28, 29]. Recently LDT has been shown to offer a route to calculating nonlinear transport coefficients [30, 31] and ways by which rare events can be made typical for engineering purposes [32].

Accessing physical properties of interest, in all but the simplest systems, requires numerical tools which arise in the form of sampling techniques such as the Cloning Algorithm or Diffusion Monte-Carlo (DMC) [33–38] and Transition Path Sampling or Path Integral Monte-Carlo [39] as well as fixed point iterative techniques such as those involving matrix product states [9, 11, 40]. Although not formally exact the latter has been very successful in accessing prototypical lattice systems using modest bond dimensions. In the absence of formal area laws it is not yet known how such techniques are applicable in general, especially in higher dimensions. Monte-Carlo techniques are generally applicable to any model and yield formally exact solutions, however, due to the growth of variance in estimators while accessing rare events, their practical use can be very limited [14, 38].

Several approaches have been suggested to tackle sampling problems that involve some form of importance sampling [10, 13, 21, 38, 41]. These techniques in their

various forms must ultimately approximate Doob’s h-transform that restores normalization to the tilted operator [42–44]. In previous work we showed that GDFs can be constructed using analytical and numerical strategies. In particular, we outlined a generalized variational principle that can be used to construct GDFs. Subsequently, we presented a procedure to construct cluster mean-field (CMF) solutions that can provide robust GDFs for many problems of interest [21, 45]. We had also suggested that the standard strategy of combining a Variational Monte-Carlo (VMC) with DMC in quantum ground state calculations is a viable strategy for computing the cumulant generating function (CGF) of Nonequilibrium Stationary States (NSS). In this paper we concretely present such a VMC + DMC hybrid technique that greatly expands the GDF construction possibilities. Before we present our method, we first outline pertinent details that are needed to understand our technique.

The central quantity of interest in large deviation theory is the cumulant generating function $\psi(\lambda)$ which is analogous to the free energy of equilibrium statistical mechanics. It is computed via a weighted ensemble average of trajectories given by,

$$\begin{aligned}\psi(\lambda) &= \lim_{t_N \rightarrow \infty} \ln \langle e^{\lambda \mathcal{O}} \rangle \\ &= \lim_{t_N \rightarrow \infty} \ln \sum_{\mathcal{C}(t_N)} P[\mathcal{C}(t_N)] e^{\lambda \mathcal{O}}\end{aligned}\quad (1)$$

where λ is a counting field conjugate to the observable $\mathcal{O} = \sum_{t=1}^{t_N} o(\mathcal{C}_{t+}, \mathcal{C}_{t-})$, with o an arbitrary function of configurations (\mathcal{C}_t) at adjacent times, $t+$ and $t-$, and t_N is the final trajectory time. $P[\mathcal{C}(t_N)]$ is the likelihood of a given trajectory $\mathcal{C}(t_N) = \{\mathcal{C}_0, \mathcal{C}_1, \dots, \mathcal{C}_{t_N}\}$. For nonequilibrium stationary states, $P[\mathcal{C}(t_N)]$ is computable from the master equation $\partial_t p_t(\mathcal{C}) = \mathcal{W} p_t(\mathcal{C})$, where $p_t(\mathcal{C})$ is the probability of a configuration of the system, \mathcal{C} , at a time t , and \mathcal{W} is a linear operator. It can be shown that

$\psi(\lambda)$ is the largest eigenvalue of a tilted operator \mathbb{W}_λ , i.e., $\mathbb{W}_\lambda|\Xi\rangle = \psi(\lambda)|\Xi\rangle$ where $|\Xi\rangle$ ($\langle\Xi|$) is the corresponding dominant right (left) eigenvector [46]. In the discrete case, $\mathbb{W}_\lambda(\mathcal{C}, \mathcal{C}') = \mathcal{W}(\mathcal{C}, \mathcal{C}')e^{\lambda\phi(\mathcal{C}, \mathcal{C}')} (1 - \delta_{\mathcal{C}, \mathcal{C}'}) - R(\mathcal{C})\delta_{\mathcal{C}, \mathcal{C}'}$, where $R(\mathcal{C}) = \sum_{\mathcal{C}' \neq \mathcal{C}} \mathcal{W}(\mathcal{C}, \mathcal{C}')$ is the exit rate.

Calculating $\psi(\lambda)$ via Monte-Carlo techniques such as the Cloning algorithm or Transition path sampling can lead to an exponentially growth of variance with $|\lambda|$ that can be greatly mitigated via auxiliary dynamics where we transform the tilted operator via an approximate Doob transformation [14, 21]:

$$\psi(\lambda) \sim \frac{1}{t_N} \ln \langle \mathbb{1} | \hat{\Xi}^{-1} [\hat{\Xi} e^{t_N \mathbb{W}_\lambda} \hat{\Xi}^{-1}] \hat{\Xi} | p_0 \rangle. \quad (2)$$

Here, the diagonal matrix $\hat{\Xi} = \sum_{\mathcal{C}} \tilde{\Xi}(\mathcal{C}) |\mathcal{C}\rangle \langle \mathcal{C}|$ is constructed from the GDF, $\langle \tilde{\Xi} | = \sum_{\mathcal{C}} \tilde{\Xi}(\mathcal{C}) \langle \mathcal{C}|$, $\langle \mathbb{1} |$ is the uniform left vector and $|p_0\rangle$ is the initial distribution of configurations. This transformation essentially partially restores the normalization of the tilted operator thereby alleviating the variance problem. The extent of the restoration is dependent on the degree of overlap between the approximate and the exact left eigenvector of \mathbb{W}_λ . The entire problem is, thus, finding appropriate GDFs to be able to compute the CGF and its associated cumulants.

As we stated earlier, our idea is to extend VMC strategies used in quantum ground state calculations to nonequilibrium classical problems [47]. We note that the energy minimization strategy in quantum VMC cannot be used here since \mathbb{W}_λ is not Hermitian. However, we can use an associated property of eigenstates, *viz.* that the variance of the quantity,

$$\Lambda(\mathcal{C}) \equiv \hat{\Xi} \mathbb{W}_\lambda |\mathcal{C}\rangle \langle \mathcal{C}| \hat{\Xi}^{-1} \quad (3)$$

must vanish for eigenstates. This quantity that we call the *local CGF*, is the analogue of the *local energy* for quantum VMC. The nonequilibrium VMC problem thus involves the minimization of

$$\sigma^2(\{p\}, \lambda) = \sum_{\mathcal{C}} w(\mathcal{C}) [\Lambda(\{p\}, \mathcal{C}) - \langle \Lambda(\{p\}) \rangle]^2, \quad (4)$$

where $\langle \Lambda(\{p\}) \rangle \equiv \sum_{\mathcal{C}} w(\mathcal{C}) \Lambda(\{p\}, \mathcal{C})$ is the average of the local CGF, $\{p\}$ are the parameters used to characterize the GDF: $\tilde{\Xi}(\{p\}, \mathcal{C})$, and $w(\mathcal{C})$ is a normalized sampling distribution. The calculation involves minimizing Eq. (4) with respect to $\{p\}$ over a fixed set of configurations $\{\mathcal{C}\}$. Once the desired level of minimization is reached a full VMC calculation can be performed with a larger set of configurations to get the final estimate of the local CGF and the variance.

Notice that (4) can be sampled from any $w(\mathcal{C})$ but for $w(\mathcal{C}) = \frac{\tilde{\Xi}(\{p\}, \mathcal{C})}{\|\tilde{\Xi}(\{p\})\|}$, $\langle \Lambda \rangle = \frac{\langle \tilde{\Xi}(\{p\}) | \mathbb{W}_\lambda | \mathbb{1} \rangle}{\langle \tilde{\Xi}(\{p\}) | \mathbb{1} \rangle}$ which is an estimator for $\psi(\lambda)$. In the absence of a bounded variational principle, the estimator of $\psi(\lambda)$ cannot rigorously be used

to judge the quality of the GDF, but in practical terms it is often useful. Whereas a strictly zero variance is guaranteed for eigenstates, smaller (non-zero) variance of the local CGF doesn't necessarily mean a better state. The more rigorous quantity is the actual reduction of the variance in the estimate of the CGF ($\varepsilon(\psi)$) from DMC or TPS. It is guaranteed that with improving quality of the GDF, $\varepsilon(\psi)$ must decrease and this is controlled by the statistical independence of samples (the trajectories which are being generated). For the cloning algorithm the indicator of statistical independence is the fraction of independent walkers (f_I) [21, 38], whereas for TPS it is the autocorrelation time (we will focus on the former, since this technique can be easily extended to the latter) [14]. Empirically f_I is seen to be less susceptible to statistical noise than $\varepsilon(\psi)$ but (for a given λ) still bears a monotonic relationship with it. It is, therefore, an excellent measure of the quality for the GDF. In the case of perfect sampling, using the exact auxiliary dynamics, f_I is equal to 1. In the other limit, if all walkers are correlated, $f_I = 0$. We note that f_I measures the correlation among walkers as a function of time, and the nature of the cloning procedure means that it must be smallest at $t = 0$ [14, 21], which is what we report. It is important to note that a small improvement in f_I might still indicate a large improvement in efficiency of the calculation. This will be evident below, where we illustrate the VMC procedure via two prototypical systems, one in the continuum and the second on the lattice.

For the continuum system, we consider the prototypical driven brownian walker, where the observable of interest is the entropy production. This system consists of $N = 10$ particles (at location $\mathbf{R} = \{r_i\}$) moving in a periodic potential ($V(r) = v_0 \cos(2\pi r)$) on a ring of size $L = 1.0$ under the influence of an external driving force (f) and a fluctuating field represented by Gaussian white noise. These particles also interact via a pairwise repulsive force ($\hat{\mathbf{f}}(r_i, r_j) = -\hat{\mathbf{f}}(r_j, r_i)$ and $|\hat{\mathbf{f}}| = \alpha \exp[-(|r_i - r_j|/r_c)^2]$). The transformed tilted propagator that includes auxiliary dynamics due to the GDF $\tilde{\Xi}(\mathbf{R})$ is given by [21],

$$\begin{aligned} \tilde{W}_\lambda &= \sum_i \partial_i (\partial_i - [\mathbf{F}_i(\mathbf{R}) \cdot \hat{\mathbf{x}} + 2f\lambda + 2 \ln \tilde{\Xi}(\mathbf{R})]) \\ &\quad + \tilde{\Xi}^{-1}(\mathbf{R}) \mathbb{W}_\lambda^\dagger \tilde{\Xi}(\mathbf{R}), \end{aligned} \quad (5)$$

where $\mathbf{F}_i(\mathbf{R}) = f\hat{\mathbf{x}} - \partial_i V(r_i)\hat{\mathbf{x}} + \sum_{j \neq i} \hat{\mathbf{f}}(r_i, r_j)$. The adjoint operator $\mathbb{W}_\lambda^\dagger = \sum_i \partial_i^2 + (\mathbf{F}_i(\mathbf{R}) \cdot \hat{\mathbf{x}} + 2f\lambda)\partial_i + f\lambda(f\lambda + \mathbf{F}_i(\mathbf{R}) \cdot \hat{\mathbf{x}})$, represents the norm breaking term that is handled via branching. Trajectories for \tilde{W}_λ is generated from the Langevin dynamics $\partial_t r_i = \mathbf{F}_i(\mathbf{R}) \cdot \hat{\mathbf{x}} + 2f\lambda + 2\partial_i \ln \tilde{\Xi}(\mathbf{R}) + \eta_i$, where the random force, η_i , satisfies $\langle \eta_i(t) \rangle = 0$ and $\langle \eta_i(t)\eta_i(t') \rangle = 2\delta(t - t')$. Note that in this formalism we have absorbed the biasing term $\exp[\lambda t_N s(t)]$ due to entropy production $s(t_N)t_N = \sum_i \int_0^{t_N} f \dot{\mathbf{r}}_i(\tau) d\tau$ into the bare Focker-Planck operator

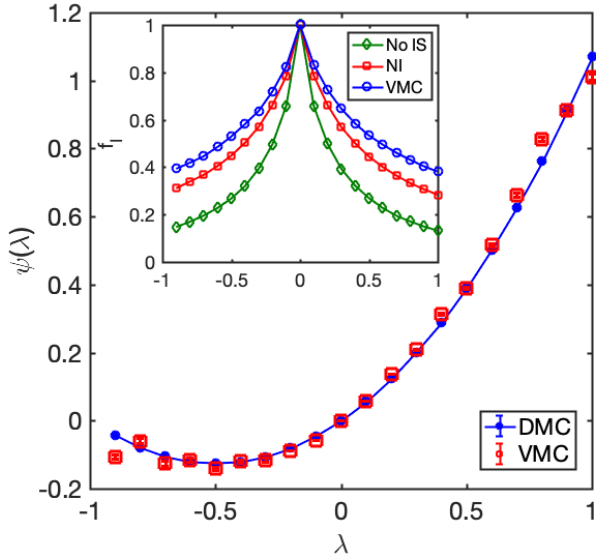


FIG. 1. Large deviation function for the entropy production of $N = 10$ driven Brownian particles on a periodic potential with $v_0 = 2$, $f = 1.0$. The Gaussian interaction force is given by $r_c = 0.10$ and $\alpha = 10.0$. The main figure shows the CGF as a function of λ computed using DMC and VMC. The DMC calculations are done with different GDF but all converge to the same estimate although the efficiencies are different. The inset shows these efficiencies measured via the fraction of independent walkers (f_I). Error bars are smaller than symbols.

[14, 21, 48].

For this system we parametrize the GDF as $\tilde{\Xi}(\mathbf{R}) = \prod_i \phi(r_i) \prod_{j < i} [J(r_i, r_j)]$, where the single particle function, $\phi(r_i)$, is obtained from the non-interacting solution generated with $M = 101$ plane wave modes [21] and $J(r_i, r_j) = \sum_{k_1, k_2} \tilde{J}(k_1, k_2) e^{ik_1 r_1 + ik_2 r_2}$. The parameters $\tilde{J}(k_1, k_2)$ are estimated using (4). Shown in Fig. 1 is the large deviation function and f_I computed using ansatz with different levels of correlation. We parametrized $J(k_1, k_2)$ with 241 parameters (21 plane waves per particle) where we used 2500 configurations and $\sigma^2(\{p\}, \lambda) < 4.0 \times 10^{-3}$ for λ 's we consider; the details relating to the specifics of the minimization procedure can be found in the supplementary information (SI) [49]. It is evident that continuum calculations can be done very efficiently with the appropriate GDFs. As noted earlier, the improvement in f_I has a number of consequences that is not apparent from the f_I comparisons alone. The actual reduction in $\varepsilon(\psi)$ can be much larger than that indicated by the improvement of f_I . For instance, the VMC generated parameters lead to no more than a $\sim 30\%$ increase in f_I relative to auxiliary dynamics with the non-interacting solution; however, the corresponding variance reduces by ~ 4 times. Additionally, although we used the same observation time to compute the CGF and cumulants for all types of sampling, the results converge much faster for simulations done with auxiliary dynamics [49].

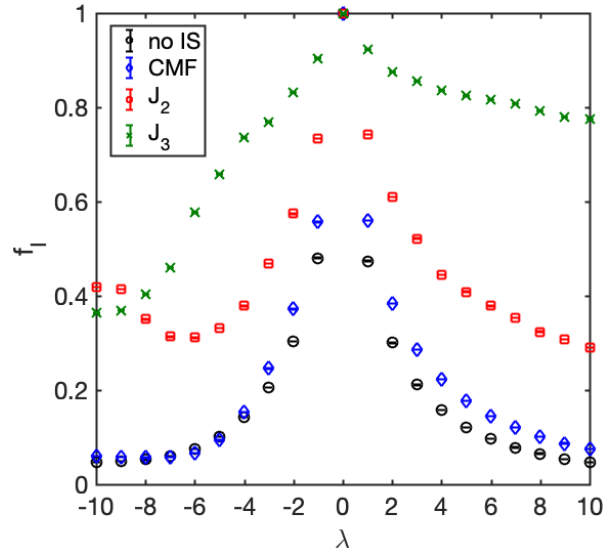


FIG. 2. Fraction of independent walkers (f_I) for different types of GDF for a $L = 16$ system. The largest degree of correlation is captured by the J_3 or three-body CPS. The VMC procedure is able to calculate the correlated amplitudes and we can systematically improve the efficiency from CMF with 8-site clusters to 2-body and 3-body CPS.

To explore our framework in different context, we now consider an interacting many-body problem on a lattice, namely the current fluctuations of a periodic weakly asymmetric simple exclusion process (WASEP) [50]. The WASEP models transport of N ($= 0.3L$) particles on a lattice with L sites, defined by a set of occupation numbers, $n_i = \{0, 1\}$, e.g. $\mathcal{C} = \{0, 1, \dots, 1, 1\}$. The tilted propagator,

$$\mathbb{W}_\lambda = \sum_{i=1}^L p e^\lambda \hat{b}_{i+1}^\dagger \hat{b}_i - p n_i (\mathbb{1} - n_{i+1}) + q e^{-\lambda} \hat{b}_{i-1}^\dagger \hat{b}_i - q n_i (\mathbb{1} - n_{i-1}) \quad (6)$$

describes the rare configurations at λ that result from particles hopping to the right with rate $p = \frac{1}{2} e^{E/L}$ and to the left with rate $q = \frac{1}{2} e^{-E/L}$. Here \hat{b}_i^\dagger (\hat{b}_i) creates (destroys) particles on site i and $n_i (\mathbb{1} - n_i)$ counts the number of particles (holes). For subsequent calculations we set $E = 10$. Periodic boundary conditions means $i = L + 1 \rightarrow 1$ and $i = 0 \rightarrow L$. Additionally hardcore constraints prevent double occupation. The weakly asymmetric limit corresponds to the Edwards-Wilkinson (EW) universality class with a dynamical critical exponent $z = 2$ [4]. This propagator is obtained by dressing the bare trajectories generated via the bare Markovian propagator by a factor of $\exp[\lambda Q(t_N)]$, where, $Q(t_N)$, is equal to the number of particle hops to the left minus the number of hops to the right,

$$Q(t_N) = \sum_{t=0}^{t_N-1} \sum_{i=0}^{L-1} \delta_{i+1}(t+1) \delta_i(t) - \delta_i(t+1) \delta_{i+1}(t) \quad (7)$$

where δ_i is the Kronecker delta function and the sum runs

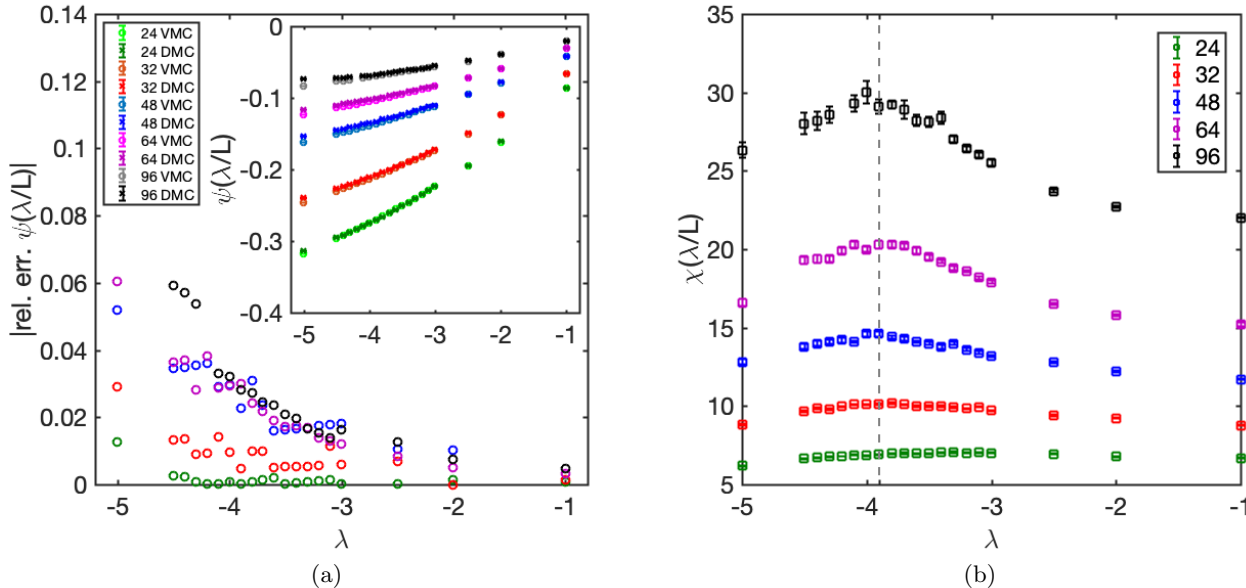


FIG. 3. (a) Relative error of VMC compared against DMC. Note that as the system size is increased and more particles are involved the GDF is unable to capture the full extent of the correlations. Nonetheless calculations still benefit from the GDF. Inset shows comparison of DMC and VMC results for the CGF ($\psi(\lambda/L)$). (b) Susceptibility ($\chi(\lambda/L)$) of the 1D WASEP for different system sizes. The dashed line at $\lambda = 3.9$ indicates possible location of the continuous phase transition in the limit of $L \rightarrow \infty$.

over the lattice site and t_N . Note that the summand is $= 0, \pm 1$ depending on particle displacement.

Unlike the continuum system, where the soft-core interaction force allows the non-interacting solution to be the starting point of constructing the GDF ansatz, the hard-core situation requires a different treatment. This system is remarkably similar to the a system of hard-core Bosons that has condensed into a superposition of low momentum plane-wave modes. This motivates building the GDF from the product of n -particle states (appropriately symmetrized with $n = 2, 3$ [49]). For instance, if $n = 2$, $\tilde{\Xi}(C) = \sum_{(i_1, \dots, i_N)} \prod_{p < q} J_2(|i_p - i_q|) [\prod_{m=1}^N b_{i_m}^\dagger] |0\rangle$ and the parameters $J_2(r)$, where r is the distance between two particles, is obtained by optimizing Eq. (4). Fig. (2) shows a comparison of $f_I(\lambda)$ for a $L = 16$ system with different GDFs. For the WASEP, the short-range CMF GDF is unable to capture the long-range correlations present in the system and therefore we do not get much improvement in the efficiency using the GDF. However, with the correlated product states (CPS) we can get large improvements (e.g., using J_3 , $\varepsilon(\psi)$ is improved by an order to two orders of magnitude [49]). We note that in these comparisons the CPS was parametrized for the full system (i.e., $|r| \leq \frac{L}{2}$).

In order to illustrate the applicability of this ansatz we undertake calculations for different system sizes $L = 24$ - 96 that were done using modest resources – the number of walkers $N_w = 10000$ to 120000 , which was enough to compute susceptibilities ($\chi(\lambda)$). For these calculations, in order to reduce the number of parameters, the GDF ansatz must be modified so that $J_3 = 1$ for $|r| > r_c = 16$

[51]. The VMC calculations used between 4000 to 8000 fixed configurations to determine 85 to 155 parameters. The accuracy of the VMC calculation has been shown in Fig. (3) where we see that the relative error grows with $|\lambda|$ as more particles become correlated. Typically for these calculations we did not spend a lot of effort in optimizing the more extreme λ values as we were interested in the range over which the susceptibility peaks where the VMC error is $< 5\%$. The spectrum of rare fluctuations in the importance sampled trajectory space (i.e. the λ space), undergoes a remarkable continuous phase transition from a uniform state to a traveling wave at some λ_c provided $E > E_c = \pi/\sqrt{\rho(1-\rho)}$ [3, 52]. This is evident from the growing susceptibility of the system that according to Macroscopic Fluctuation Theory (MFT) diverges at $\lambda_c = -E + \sqrt{E^2 - E_c^2} = -2.7198$ (for $\rho = 0.3$). However, MFT is not quantitatively accurate outside $E \sim E_c$ and although a Bethe Ansatz formulation exists the precise value of λ for $L \rightarrow \infty$ is not explicitly known [4]. Our DMC calculations suggest that the critical point is $\lambda_c \sim 3.9$ for the largest system sizes ($L = 64, 96$). We note that our results for $\psi(\lambda/L)$ are in excellent agreement with system sizes considered in [52].

In this article we have shown GDFs can be computed using a VMC procedure that minimizes the variance of the local CGF. The quality of the GDF can be readily gauged using the f_I measure from DMC or the auto-correlation time from TPS. We have shown that the VMC procedure is very robust and works with relatively general parametrizations of the GDF. Additionally it is much less expensive compared to DMC. For instance, in the

case of the 1D Brownian walker VMC needs a relatively small number of configurations (~ 2500 - 10000) relative to DMC that generates $\sim 5,000,000$ configurations over the integration time (typically DMC requires multiple integration sweeps to compute the CGF). This makes the VMC+DMC hybrid approach a powerful way to handle non-equilibrium systems of interest. The additional advantage of this approach is that GDFs can be constructed by systematically incorporating different levels of correlation. We illustrated such an approach in the 1D Brownian walker where we combined solutions from non-interacting systems together with two-body correlator ansatz that is computed by optimizing the GDF via VMC. The CPS construction for the 1D WASEP, on the other hand, shows how GDFs can be calculated directly from VMC incorporating different levels of correlations and symmetries. The general form of the VMC variance minimization function (Eq. (4)) can be applied to any problem of interest and, therefore, opens up the possibility to access more complex systems.

Acknowledgements: The authors would like to thank Rob Jack, Vivien Lecomte, Juan P. Garrahan and David Limmer for fruitful and engaging discussions. U. R. was supported by the Simons Collaboration on the Many-Electron Problem and the California Institute of Technology. G. K.-L. C. is a Simons Investigator in Theoretical Physics and was supported by the California Institute of Technology and the US Department of Energy, Office of Science via DE-SC0018140. These calculations were performed with CANSS, available at <https://github.com/ushnishray/CANSS>.

* uray@caltech.edu

† garnetc@caltech.edu

- [1] H. Touchette, *Physics Reports* **478**, 1 (2009).
- [2] B. Derrida, J. L. Lebowitz, and E. R. Speer, *Journal of Statistical Physics* **110**, 775 (2003).
- [3] T. Bodineau and B. Derrida, *Physical Review E* **72**, 066110 (2005).
- [4] S. Prolhac and K. Mallick, *Journal of Physics A: Mathematical and Theoretical* **42**, 175001 (2009).
- [5] J. de Gier and F. H. L. Essler, *Phys. Rev. Lett.* **107**, 010602 (2011).
- [6] P. I. Hurtado and P. L. Garrido, *Physical review letters* **107**, 180601 (2011).
- [7] M. Gorissen, A. Lazarescu, K. Mallick, and C. Vanderzande, *Phys. Rev. Lett.* **109**, 170601 (2012).
- [8] A. Lazarescu, *Journal of Physics A: Mathematical and Theoretical* **48**, 503001 (2015).
- [9] P. Helms, U. Ray, and G. K.-L. Chan, *Phys. Rev. E* **100**, 022101 (2019).
- [10] T. Nemoto, R. L. Jack, and V. Lecomte, *Physical Review Letters* **118**, 115702 (2017).
- [11] M. C. Bañuls and J. P. Garrahan, arXiv e-prints , arXiv:1903.01570 (2019), arXiv:1903.01570 [cond-mat.stat-mech].
- [12] S. Whitelam, L. O. Hedges, and J. D. Schmit, *Physical review letters* **112**, 155504 (2014).
- [13] K. Klymko, P. L. Geissler, J. P. Garrahan, and S. Whitelam, arXiv:1707.00767 (2017).
- [14] U. Ray, G. K.-L. Chan, and D. T. Limmer, *The Journal of Chemical Physics* **148**, 124120 (2018).
- [15] R. L. Jack, *Phys. Rev. E* **100**, 012140 (2019).
- [16] A. Prados, A. Lasanta, and P. I. Hurtado, *Phys. Rev. Lett.* **107**, 140601 (2011).
- [17] A. Prados, A. Lasanta, and P. I. Hurtado, *Physical Review E* **86**, 355 (2012).
- [18] J. Mehl, T. Speck, and U. Seifert, *Physical Review E* **78**, 011123 (2008).
- [19] R. Chetrite and H. Touchette, *Journal of Statistical Mechanics: Theory and Experiment* **2015**, P12001 (2015).
- [20] P. Tsobgni Nyawo and H. Touchette, *Phys. Rev. E* **94**, 032101 (2016).
- [21] U. Ray, G. K.-L. Chan, and D. T. Limmer, *Physical Review Letters* **120**, 210602 (2018).
- [22] T. GrandPre and D. T. Limmer, *Phys. Rev. E* **98**, 060601 (2018).
- [23] O. Shpielberg, T. Nemoto, and J. a. Caetano, *Phys. Rev. E* **98**, 052116 (2018).
- [24] J. Dolezal and R. L. Jack, arXiv e-prints , arXiv:1906.07043 (2019), arXiv:1906.07043 [cond-mat.stat-mech].
- [25] N. Tizón-Escamilla, V. Lecomte, and E. Bertin, *Journal of Statistical Mechanics: Theory and Experiment* **2019**, 013201 (2019).
- [26] T. Nemoto, E. Fodor, M. E. Cates, R. L. Jack, and J. Tailleur, *Phys. Rev. E* **99**, 022605 (2019).
- [27] K. Proesmans and B. Derrida, *Journal of Statistical Mechanics: Theory and Experiment* **2019**, 023201 (2019).
- [28] F. Carollo, J. P. Garrahan, and I. Lesanovsky, *Phys. Rev. B* **98**, 094301 (2018).
- [29] A. J. Schile and D. T. Limmer, *The Journal of Chemical Physics* **149**, 214109 (2018), <https://doi.org/10.1063/1.5058281>.
- [30] C. Y. Gao and D. T. Limmer, arXiv e-prints , arXiv:1812.01470 (2018), arXiv:1812.01470 [cond-mat.stat-mech].
- [31] U. Ray and D. T. Limmer, arXiv e-prints , arXiv:1906.11429 (2019), arXiv:1906.11429 [cond-mat.mes-hall].
- [32] F. Carollo, J. P. Garrahan, I. Lesanovsky, and C. Pérez-Espigares, *Phys. Rev. A* **98**, 010103 (2018).
- [33] P. Grassberger, *Computer Physics Communications* **147**, 64 (2002).
- [34] P. Del Moral and J. Garnier, *Ann. Appl. Probab.* **15**, 2496 (2005).
- [35] C. Giardinà, J. Kurchan, and L. Peliti, *Phys. Rev. Lett.* **96**, 120603 (2006).
- [36] C. Giardinà, J. Kurchan, V. Lecomte, and J. Tailleur, *Journal of statistical physics* **145**, 787 (2011).
- [37] F. Crou, A. Guyader, T. Lelivre, and D. Pommier, *The Journal of chemical physics*, **134**, 054108 (2011).
- [38] T. Nemoto, F. Bouchet, R. L. Jack, and V. Lecomte, *Phys. Rev. E* **93**, 062123 (2016).
- [39] P. G. Bolhuis, D. Chandler, C. Dellago, and P. L. Geissler, *Annual review of physical chemistry* **53**, 291 (2002).
- [40] M. Gorissen, J. Hooyberghs, and C. Vanderzande, *Physical Review E* **79**, 020101 (2009).
- [41] D. Jacobson and S. Whitelam, arXiv e-prints , arXiv:1903.06098 (2019), arXiv:1903.06098 [cond-

- mat.stat-mech].
- [42] J. L. Doob, *Classical Potential Theory and Its Probabilistic Counterpart* (Springer-Verlag, 1984).
- [43] R. Chetrite and H. Touchette, in *Annales Henri Poincaré*, Vol. 16 (Springer, 2015) pp. 2005–2057.
- [44] R. L. Jack and P. Sollich, *Progress of Theoretical Physics Supplement* **184**, 304 (2010).
- [45] U. Ray and D. T. Limmer, *The Journal of Chemical Physics* (2019).
- [46] J. L. Lebowitz and H. Spohn, *Journal of Statistical Physics* **95**, 333 (1999).
- [47] C. J. Umrigar, K. G. Wilson, and J. W. Wilkins, *Phys. Rev. Lett.* **60**, 1719 (1988).
- [48] U. Seifert, *Reports on Progress in Physics* **75**, 126001 (2012).
- [49] See Supplemental Material for the transformed tilted operator for the continuum, forms of the GDF along with the necessary symmetries used in the VMC procedure, details of the ways in which the statistical efficiency of the computations are improved via auxiliary dynamics, and some relevant details of the VMC minimization.
- [50] B. Schmittmann and R. K. Zia, *Phase transitions and critical phenomena* **17**, 3 (1995).
- [51] See Supplemental Material for more details on CPS setup [49]. Since calculations are expensive with such large systems, we estimate the smallest gain in efficiency is $f_I/f_I^0 \sim 4$ for $L = 96$ at $\lambda = -5$. For smaller system and larger λ , f_I/f_I^0 will be larger.
- [52] C. P. Espigares, P. L. Garrido, and P. I. Hurtado, *Physical Review E* **87**, 032115 (2013).

Constructing Auxiliary Dynamics for Nonequilibrium Stationary States with Variational Monte-Carlo: Supplementary Information

Ushnish Ray* and Garnet Kin-Lic Chan†
 Division of Chemistry and Chemical Engineering,
 California Institute of Technology, Pasadena, CA 91125
 (Dated: April 1, 2022)

GUIDING DISTRIBUTION FUNCTION CONSTRUCTION FOR THE CONTINUUM

In the main text we have mentioned that computing the cumulant generating function (CGF) of 1D continuum system can be greatly enhanced with the appropriate form of auxiliary dynamics. The structure we have introduced is of the form $\tilde{\Xi}(\mathbf{R}) = \prod_i \phi(r_i) \prod_{j < i} [J(r_i, r_j)]$ so that that one and two-particle ansatz can be parameterized independently. This is particularly useful for continuum systems as we must typically represent each of these functions in a basis of known functions such as plane-waves. By writing the functions in this form every additional level of correlation can be handled with different basis or sizes. For the adjoint of the Focker-Planck operator considered in the main text we can show that,

$$\begin{aligned} \frac{\mathbb{W}_\lambda^\dagger \tilde{\Xi}(R)}{\tilde{\Xi}(R)} = & \sum_{i=1}^N \left\{ \frac{P_1^\dagger \phi(r_i)}{\phi(r_i)} + \sum_{j \neq i} \frac{\partial^2 J(r_i, r_j)}{\partial r_i^2} + \right. \\ & \left[\gamma_i(r_i) + 2\lambda + \frac{2}{\phi(r_i)} \frac{d\phi(r_i)}{dr_i} \right] \left[\sum_{j \neq i} \frac{\partial J(r_i, r_j)}{\partial r_i} \right] + \\ & \left. \left[\sum_{j \neq i} \hat{\mathbf{f}}(r_i, r_j) \cdot \hat{\mathbf{x}} \right] \left[\frac{1}{\phi(r_i)} \frac{d\phi(r_i)}{dr_i} + \sum_{j \neq i} \frac{\partial J(r_i, r_j)}{\partial r_i} \right] \right\}. \end{aligned} \quad (\text{S1})$$

Here, the non-interacting single-particle operator is given by,

$$\begin{aligned} \frac{P_1^\dagger \phi(r_i)}{\phi(r_i)} = & \frac{1}{\phi(r_i)} \frac{d\phi(r_i)}{dr_i} + \frac{\gamma_i(r_i) + 2\lambda}{\phi(r_i)} \frac{d\phi(r_i)}{dr_i} \\ & + \lambda(\lambda + \gamma_i(r_i)) \end{aligned} \quad (\text{S2})$$

where $\gamma_i(r_i) = f - \partial_i V(r_i)$ is the effective single-particle force acting on a particle. With these expressions we can evaluate the norm breaking term in DMC for the given form of auxiliary dynamics. It is straightforward to generalize these expressions to higher dimensions.

GUIDING DISTRIBUTION FUNCTION CONSTRUCTION FOR 1D WASEP

For the 1D WASEP consisting of hard-core particles interacting on a lattice, we use correlated product states

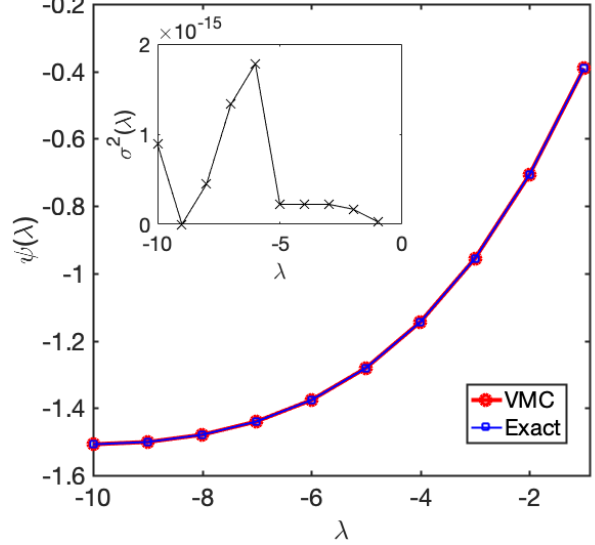


FIG. S1. CGF computed using exact diagonalization and VMC for a 1D WASEP system with $N = 3$ particles, $L = 8$ system with periodic boundary conditions. The VMC calculations were done using the J_3 GDF, which must be exact (see text). Inset shows the VMC estimate of the variance of the local CGF, which is converged to $< 2.0 \times 10^{-15}$ for any λ .

(CPS) for auxiliary dynamics. When using the two-particle correlators the ansatz takes the form,

$$\tilde{\Xi}(C) = \sum_{(i_1, \dots, i_N)} \prod_{p < q} J_2(|i_p - i_q|) \left[\prod_{m=1}^N b_{i_m}^\dagger \right] |0\rangle, \quad (\text{S3})$$

which is of the form of the Gutzwiller ansatz for hard-core Bosonic condensate. This is evident from $\sum_{\{i_p\}} \left[\prod_{n=1}^N b_{i_n}^\dagger \right] |0\rangle = \hat{\mathbb{P}}(b_{k=0}^\dagger)^N |0\rangle$, where $\hat{\mathbb{P}}$ projects out all possible double and higher order occupation of a particular site from a $k = 0$ non-interacting condensate. This is a quintessential hard-core Bosonic condensate which forms the dominant left eigenvector or the solution to the 1D WASEP for $\lambda = 0$. The modulation introduced by $J_2(r)$ leads to depletion of the hard-core condensate for other values of $|\lambda| > 0$ but introduces spatially dependent correlations. As noted in the main text, higher order correlations can be introduced by using higher order CPS. For our computations we additionally used a three-body CPS given by $J_3(i_p, i_q, i_r)$.

The periodic boundary conditions and translational invariance in the system introduces symmetries that can be

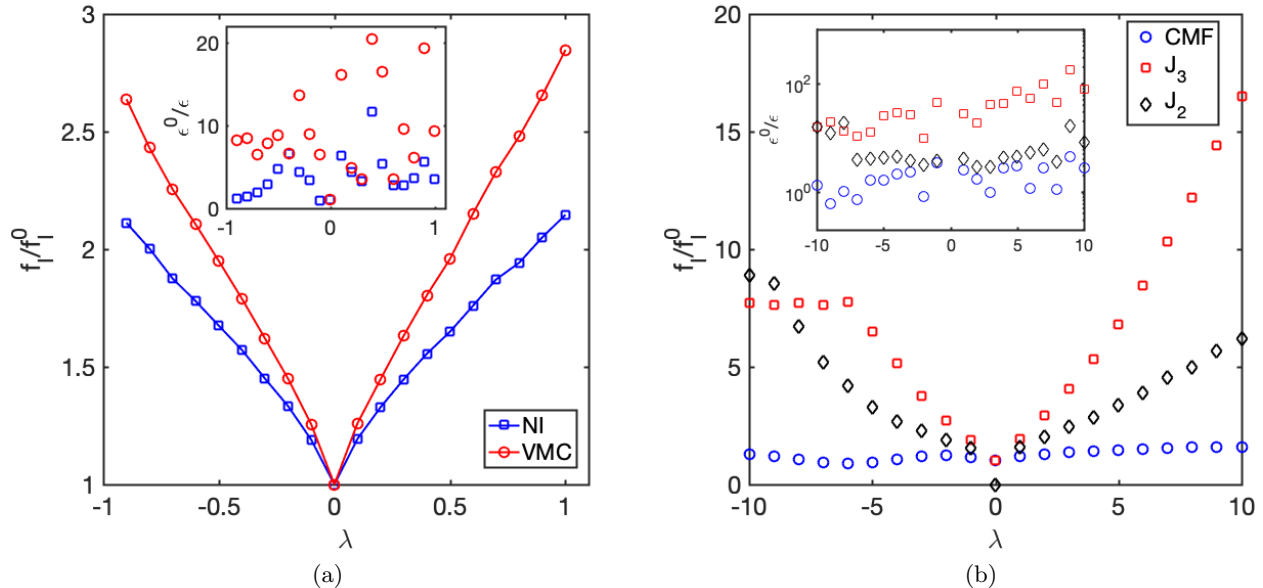


FIG. S2. Improvement in the fraction of independent walkers (f_I) relative to calculations done without any auxiliary dynamics (f_I^0) for (a) 1D Brownian walker (b) 1D WASEP. Error bars are smaller than symbol sizes. The inset shows the corresponding improvement in the variance of the CGF ($\epsilon(\psi)$). No error estimate available for the variances (see text).

exploited to reduce the number of parameters that VMC must optimize. Additionally it also produces GDF that respect the symmetries of the system which is important, since the VMC procedure must optimize the variance of the CGF given the constraints. The two particle case is straightforward and all that is needed is we map $|i_p - i_q|$ to the smallest distance around the ring, i.e., $J_2 = J_2(\min(|i_p - i_q|, L - |i_p - i_q|))$. For large systems we additionally require that $J_2(|r|) = 1.0$ for $|r| > r_c$. Notice that by utilizing the symmetry of the system we have reduced the $L/2\mathbb{C}_2$ possible parameters to just $L/2$ parameters for optimization (if $r_c = L/2$).

In the three-body case the symmetrization can be achieved in the following way: we map $(i_p, i_q, i_r) \rightarrow \mathbb{O}(\min(|i_p - i_q|, L - |i_p - i_q|), \min(|i_p - i_r|, L - |i_p - i_r|), \min(|i_q - i_r|, L - |i_q - i_r|)) = (a, b, c)$. Here \mathbb{O} orders the 3-tuple in some way, for example in ascending order so that $a \leq b \leq c$. All cyclic permutations of 3-tuple map to same value. If any two or more 3-tuple values are equal, then cyclic and anti-cyclic permutations also map to the same value. Fig. (S1) shows results from VMC and exact results for a system of size $L = 8$ with $N = 3$ particles using J_3 . As expected, in this case the J_3 function parametrizes the exact GDF and so VMC is able to reduce the variance of the local CGF ($\sigma^2(\{p\}, \lambda)$) to 0.

We can also restrict correlations to finite distances $J_3(a, b, c) = J_2(a, b)J_2(a, c)J_2(b, c)$, i.e., we map the 3-body correlations to 2-body correlations if $\exists x \in (a, b, c)$ $x > r_c$. An even simpler form is $J_3(a, b, c) = 1.0$, if $\exists x \in (a, b, c)$ $x > r_c$. These two conditions can be further combined and we can define two distances (r_{c1} and r_{c2}) so that we progress from three-body to two-body

correlations for $r_{c1} < r \leq r_{c2}$, and finally no correlation for $r > r_{c2}$. For the results we presented for the large system we only use the simple form.

STATISTICAL INDEPENDENCE AND EFFICIENCY IMPROVEMENT WITH AUXILIARY DYNAMICS

In the main text we have mentioned that an improvement of the GDF is indicated by the improvement in the fraction of independent walker (f_I) estimated from DMC (and a corresponding decrease in the autocorrelation time for TPS). One important consequence of that improvement is the reduction in the variance of the CGF as estimated from DMC. Fig. (S2) shows the improvement in f_I relative to calculations done without any auxiliary dynamics for the 1D Brownian walker and the 1D $L = 16$ WASEP system. Although it is difficult to accurately measure the factor improvement in the variance (since the variance are small numbers and subject to statistical noise), the inset of Fig. (S2) shows the corresponding improvement in variance relative to the variance of CGF calculated from no importance sampling. Notice the massive improvement in efficiency over the range of λ using GDFs. These improvements result from the fact that the computations are done over trajectories (or finite projection time) and the benefit from auxiliary dynamics extend throughout that time (recall that we have only reported f_I for $t = 0$ in the main text). This is evident from the full $f_I(t)$ shown in Fig. (S3) for calculations done using different auxiliary dynamics forms at $\lambda = -5.0$ for the

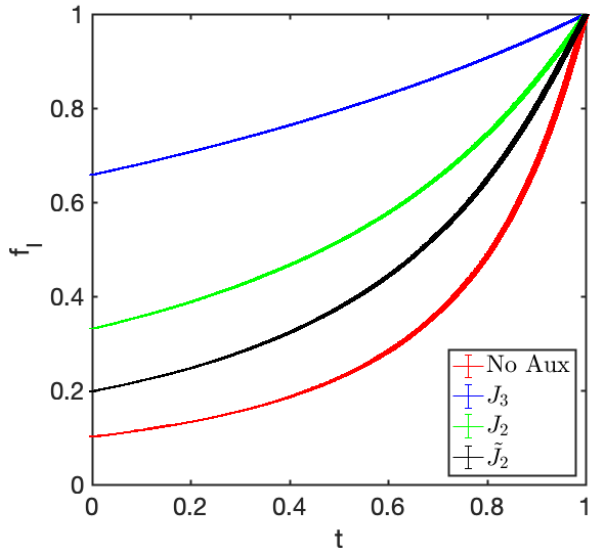


FIG. S3. Fraction of independent walkers (f_I) as a function of normalized observation time for different types of auxiliary dynamics for $\lambda = -5.0$. (See text)

1D WASEP system. The two two-body forms of auxiliary dynamics, J_2 and \tilde{J}_2 , are from two VMC calculations where the J_2 parameters were obtained by allowing the VMC to search for longer time so that the corresponding GDFs were of higher quality (evidenced from the $f_I(t)$ comparisons of Fig. (S3)). There is also another not so obvious improvement in the systematic error due to finite population of walkers. As seen in Table (I), the expectation value of the CGF moves towards estimates with lower bias as the GDF becomes more accurate. Additionally, the variance is systematically improved.

VMC OPTIMIZATION DETAILS

In this work we perform the VMC optimization using a simple simplex based algorithm found in the GNU Scientific Library package. This can be modified to more sophisticated procedure such as stochastic gradient, which will allow larger number of parameters to be utilized. However, for illustration purposes, the method we use turns out to be sufficient. For the continuum system, Fig. (S4) shows a trace of the variance $\sigma^2(\{p\}, \lambda)$ at $\lambda = -0.5$

GDF	$\psi(\lambda)$	$\varepsilon(\lambda)$
No Aux	-0.5012	1.3e-04
\tilde{J}_2	-0.50113	9.2e-05
J_2	-0.50106	2.9e-05
J_3	-0.501049	4.9e-06

TABLE I. CGF estimate and variance for different auxiliary dynamics at $\lambda = -0.5$ (see text).

produced by the minimization procedure, along with the local CGF estimator shown in the inset. This is generally how the minimization proceeds. For this trace we started the minimization from $J(k_1 = 0, k_2 = 0) = 1.0$ and all other parameters set to 0. The corresponding variance estimates was $1.0 \times 10^{-4} < \sigma^2(\{p\}) < 4.0 \times 10^{-3}$. We note that for $-0.3 \leq \lambda \leq 0.3$ ($\lambda \neq 0.0$) there were local minima issues, which were resolved by increasing the number of configurations from 2500 to 10000 configurations. If $\Delta\lambda$ for the range we consider is small then another strategy is to use adjacent converged calculations as the initial guess for the current minimization. This is the strategy we pursue with the 1D WASEP system, which produces very tight estimates for the VMC calculations as seen in the main text. The corresponding variance estimates satisfied $8.5 \times 10^{-8} < \sigma^2(\{p\}, \lambda) < 1.0 \times 10^{-6}$ for $L = 96$. These calculations were done using 8000 configurations.

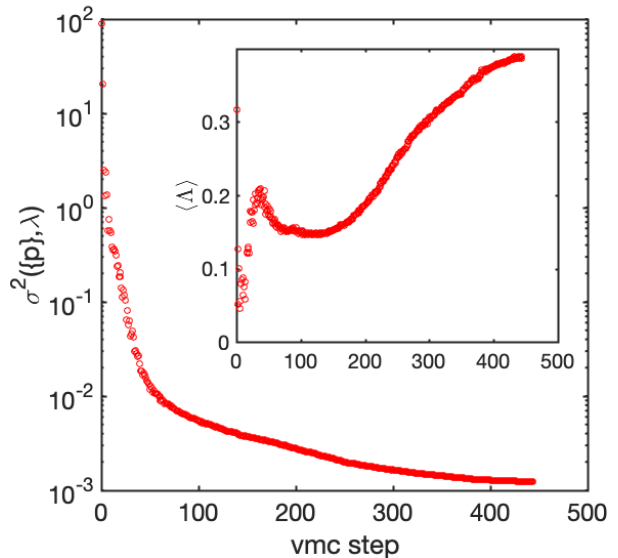


FIG. S4. VMC minimization trace of continuum system for $\lambda = 0.5$. Inset shows how the local CGF changes as the minimization proceeds (see text).